Tryptophan Interactions in Bacteriorhodopsin: A Heteronuclear Solid-State NMR Study†

Aneta T. Petkova,‡,§ Minoru Hatanaka,§ Christopher P. Jaroniec,§ Jingui G. Hu,‡,§ Marina Belenky,‡ Michiel Verhoeven,|| Johan Lugtenburg,|| Robert G. Griffin,§ and Judith Herzfeld*,‡

Department of Chemistry and Keck Institute for Cellular Visualization, MS #015, Brandeis University, Waltham, Massachusetts 02454-9110, Francis Bitter Magnet Laboratory and Department of Chemistry, Massachusetts Institute of Technology, Cambridge, Massachusetts 02139, and Rijksuniversiteit te Leiden, 2300 RA Leiden, The Netherlands

Received December 6, 2001

ABSTRACT: The bulky and amphiphilic nature of tryptophan residues makes them particularly interesting components of proteins. In bacteriorhodopsin, four of the eight tryptophan residues are in the active site, forming parts of the retinal binding pocket. In this work, we use solid-state NMR to study the interactions of the tryptophan residues in wild-type bacteriorhodopsin, in the resting state, and in critical intermediates of the proton-motive photocycle. The range of the chemical shifts of the indole nitrogens suggests that all eight of them are hydrogen bonded. Using difference spectroscopy, we isolate several changes in these hydrogen bonds in the early and late M states. As found earlier for the peptide backbone, some perturbations found in the early M state relax in the transition to the late M state while new perturbations arise. Interestingly, Rotational Echo DOuble Resonance (REDOR) difference spectroscopy of [20-^{13}C]retinal,-[*indole*-^{15}N]Trp-bR shows that indole of Trp182 is not involved in the significant hydrogen bond perturbations. We also use REDOR to measure dipolar interactions in [20-^{13}C]retinal,[*indole*-^{15}N]Trp-bR, and thereby determine the distance between the C_{20} of retinal and the indole nitrogen of Trp182. The internuclear distance changes only slightly from the light-adapted state (3.36 ± 0.2 Å) to the early M state (3.16 ± 0.4 Å).

Bacteriorhodopsin (bR)[1] is a retinal pigment that functions as a light-driven proton pump in the cell membranes of *Halobacterium salinarum*. Intermediates in the proton-motive photocycle with distinct absorption spectra are labeled sequentially as bR_{568} (or LA), J, K, L, M, N, and O. The photocycle begins with photoinduced isomerization of the retinal chromophore from all-trans,15-anti to 13-cis,15-anti. Subsequent deprotonation of the Schiff base (SB) that links the retinal to Lys216 (in the L→M transition) is coupled to protonation of Asp85 and the eventual release of a proton from a complex of residues at the extracellular surface. On the other hand, proton uptake occurs at the cytoplasmic side of the membrane, after Asp96 has donated its proton to the SB (in the M→N transition). The reprotonated chromophore then reisomerizes from 13-cis,15-anti to all-trans,15-anti, and Asp85 deprotonates to recover the initial state [see references (*1*−*3*)].

Although considerable progress has been made toward elucidating the detailed proton transfer mechanism in bR, many key issues remain unresolved. Primary among them is the means by which backflow is prevented. Thus, much attention has focused on differences between the early M state in which the SB proton has just been released to the extracellular side of the protein and the late M state in which the SB is about to be reprotonated from the intracellular side of the protein. Multiple M intermediates have been predicted by molecular dynamics simulations (*4*−*6*) and by different sequential kinetic schemes to which time-resolved visible absorption profiles were fitted (*7*, *8*). It was also found that in various bR preparations, two successive M's could be distinguished by a 4−7 nm blue shift in the absorption (*7*, *9*). However, FTIR studies have so far found only very small variations in the M intermediates in native bR (*10*).

Recently we (*11*) succeeded in distinguishing early M (M_o) and late M (M_n) photocycle intermediates in solid-state nuclear magnetic resonance (SSNMR) magic angle spinning (MAS) spectra. The M_o and M_n states were accumulated at different temperatures and shown to comply with the scheme

† This research was supported by the National Institutes of Health (Grants GM-36810, GM-23289, and RR-00995). C.P.J. was supported by a Predoctoral Fellowship from the National Science Foundation.

* To whom correspondence should be addressed. Voice: 617-736-2538. Fax: 617-736-2516. E-mail: herzfeld@brandeis.edu.

‡ Brandeis University.

§ Massachusetts Institute of Technology.

|| Rijksuniversiteit te Leiden.

[1] Abbreviations: bR, bacteriorhodopsin; bR_{568}, the all-trans,15-anti component of dark-adapted bR and the sole component of light-adapted bR; bR_{555}, the 13-cis,15-syn component of dark-adapted bR; CP, cross-polarization; CW, continuous wave; DA, dark-adapted state of bR, an ∼1:2 mixture of bR_{568} and bR_{555}; DSS, 2,2-dimethyl-2-silapentane-5-sulfonate, sodium salt; Gdn-HCl, guanidine hydrochloride; FTIR, Fourier transform infrared; LA, light-adapted state of bR; L, intermediate in the bR_{568} photocycle in which the SB is still protonated; M_o and M_n, successive intermediates in the bR_{568} photocycle in which the SB is deprotonated; N and O, successive photocycle intermediates in which the SB is reprotonated; MAS, magic angle spinning; NMR, nuclear magnetic resonance; REDOR, rotational echo double resonance; SB, Schiff base; SSNMR, solid-state NMR; TMS, tetramethylsilane; TPPM, two-pulse phase modulation; WT, wild type.

10.1021/bi012127m CCC: $22.00
Published on Web 01/25/2002

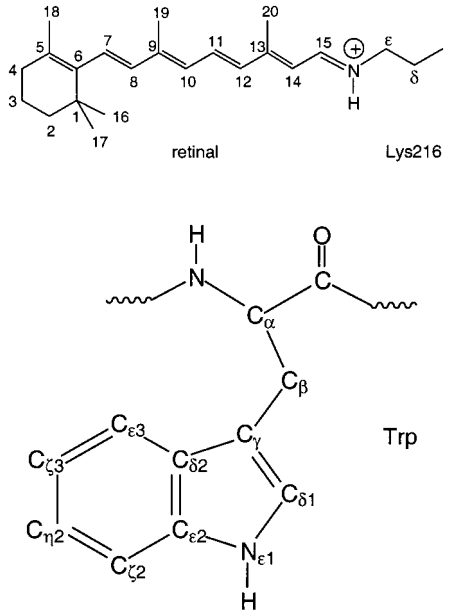

FIGURE 1: Structure and nomenclature for the retinal Schiff base and tryptophan.

$bR_{568} \rightarrow L \rightarrow M_o \rightarrow (M_n+N) \rightarrow bR_{568}$. Both M intermediates have a 13-cis,15-anti conformation as determined from the chemical shifts of C_{12} and C_{14} in the retinal (for nomenclature, see Figure 1) and C_ϵ in Lys216. However, the ^{15}N chemical shift of the SB moves upfield by about 8 ppm in the $M_o \rightarrow M_n$ transition. This shift indicates an increase in the pK_a and/or hydrogen bonding of the SB, and therefore greater readiness to reprotonate. Furthermore, the contrast with the blue shift in the visible spectrum indicates that the relaxation of chromophore distortion between the L and N states can be localized to the $M_o \rightarrow M_n$ transition (*12*). In addition, the $M_o \rightarrow M_n$ transition is associated with significant changes in the protein backbone (*11*). Given the observed changes in the SB, the chromophore, and the peptide backbone, it seems likely that the $M_o \rightarrow M_n$ transition serves as the "reprotonation switch" of the bR photocycle.

Tryptophan has the bulkiest side chain of all the amino acids, and shows both hydrophobic properties (through the aromatic system) and hydrophilic properties (through the indole nitrogen). The replacement of tryptophan with other amino acid residues thus may induce significant changes in protein function. bR has eight tryptophan residues, and four of them, Trp86, Trp138, Trp182, and Trp189, are part of the retinal binding pocket (*13, 14*). In particular, Trp86 and Trp182 sandwich the polyene chain, while Trp138 and Trp189 are close to the β-ionone ring (see Figure 2).

Trp86 is located near Asp85, and is thought to affect the hydrogen bonding system around the SB in the first step of the photocycle (*15*). Furthermore, it has been suggested that Trp86 inhibits dark adaptation (i.e., the thermal isomerization of the chromophore from all-*trans*,15-*anti*-retinal to 13-*cis*,-15-*syn*-retinal) (*15*) and causes the retinal to be distorted from a planar structure in the light-adapted state (*16*). FTIR studies of WT, W182F, and 9-desmethylretinal bR (*17*) have found that Trp182, which is situated in the cytoplasmic half of helix F, interacts with the retinal chromophore via the C_9 methyl group, and that Trp182 plays a role in the L→M transition. Time-resolved UV−vis and pH measurements, and static and time-resolved FTIR studies of WT, W182F, and 9-desmethylretinal bR (*18*) have shown that the steric interaction between Trp182 and the C_9 methyl group is important for retinal reisomerization (13-cis→all-trans) and proton transfer in the late part of the bR photocycle. UV and visible resonance Raman data of WT and W182F (*19*) suggest an unusually strong interaction between the indole ring of Trp182 and both the C_9 and C_{13} methyl groups of the retinal.

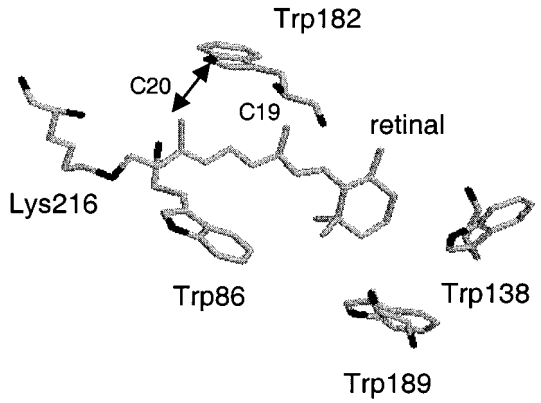

FIGURE 2: Representation of the tryptophan residues surrounding the retinal based on X-ray diffraction results (*58*).

Both hydrogen bonding and steric interactions can be probed with great sensitivity by nuclear magnetic resonance (NMR). Here we use solid-state NMR to study intact purple membranes labeled with ^{13}C at C_{20} of the retinal and ^{15}N in the indole rings of the tryptophan residues. The [*indole*-^{15}N] chemical shifts report hydrogen bond strengths, and the $^{15}N-^{13}C$ dipolar interaction allows assignment of the [*indole*-^{15}N]-Trp182 signal and measurement of the [20-^{13}C]retinal-to-[*indole*-^{15}N]Trp182 internuclear distance. Changes during proton pumping are followed by thermal trapping of critical intermediates in the photocycle.

MATERIALS AND METHODS

Model Compounds. Crystalline Trp-Gly-Gly·$2H_2O$, Ac-Trp-OMe, L-tryptophan picrate, *N*-methyl-L-tryptophan, and Trp·HBr were prepared from the natural-abundance ingredients (Sigma Chemical Co., St. Louis, MO) following the procedures outlined in the respective structure determination papers (*20*−*24*).

[20-^{13}C]Retinal,[indole-^{15}N]Trp-bR. [20-^{13}C]Retinal was synthesized as described previously (*25*). [*indole*-^{15}N]Trp-bR was prepared by growing the JW-3 strain of *Halobacterium salinarum* in a synthetic medium (*26*) containing [^{15}N]anthranilic acid instead of natural-abundance L-tryptophan. Co-incorporated [U-^{14}C]anthranilic acid was used as a radioactive tracer. The purple membranes were isolated and purified in the usual manner (*27*). Extraction found negligible radioactivity (3−6%) in the lipids and chromophore. Labeling of the tryptophan residues was estimated at 63%. ^{15}N label not in tryptophan was expected to be redistributed between the amide nitrogens and the η-nitrogens of the arginine side chains since the biochemical degradation of anthranilic acid would transfer the label directly to ammonia. [*indole*-^{15}N]Trp-bR was reconstituted with [20-^{13}C]retinal according to the procedure described in (*11*). [20-^{13}C]Retinal,[*indole*-^{15}N]Trp-bR was washed several times with 0.3 M Gdn-HCl at pH 10, and a pellet containing about 30 mg of bR was packed in a transparent quartz rotor (Wilmad Glass Co., Buena, NJ).

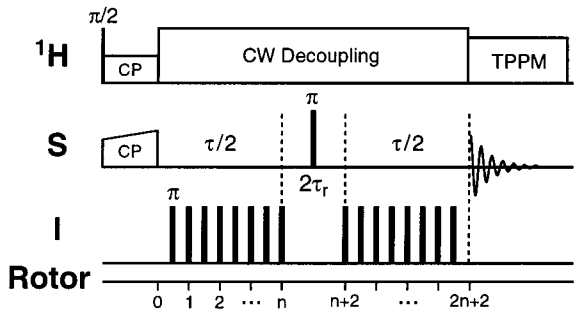

FIGURE 3: Rotational echo double resonance (REDOR) pulse sequence (*31*). The S-spins are cross-polarized from the ^{1}H reservoir, and the signal is observed as a spin−echo. The rotor-synchronized π pulses (one pulse every $1/2\tau_r$) applied to the I nuclei reintroduce the I−S dipolar couplings. The I-spin pulses were phased according to the xy-8 scheme (*33*) to minimize pulse imperfections. To account for relaxation effects, a reference (S_0) experiment was recorded for each REDOR (S) experiment, by acquiring the spectrum in the absence of I-spin π pulses.

Photocycle Intermediates. The bR photocycle intermediates were accumulated in situ. The light-adapted (LA) state was obtained from the dark-adapted state via white light illumination (1000 W Xe lamp, Oriel Instruments, Stratford, CT) for 4 h at 2 °C, or upon thermal relaxation of LA photoproducts at 0 °C for 1 h. The M_o and M_n intermediates were accumulated by illumination of LA at −60 and −20 °C, respectively, with $\lambda > 530$ nm (long-pass filter from Oriel Instruments) for 2 h. Once accumulated, all intermediates were cryo-trapped at −90 °C, where NMR data were acquired in the dark.

Solid-State NMR Spectroscopy. The NMR experiments were performed on custom-designed spectrometers (courtesy of Dr. D. J. Ruben) operating at ^{1}H Larmor frequencies of 317 and 400 MHz, with quadruple- and triple-resonance transmission line MAS probes (designed by Dr. C. M. Rienstra), equipped with 5 and 4 mm Chemagnetics spinner modules, respectively. The ^{13}C chemical shifts are referenced to TMS with adamantane as a secondary standard [resonances at 38.56 and 29.50 ppm (*28*)]. The ^{15}N chemical shifts are referenced to virtual liquid NH_3 by using the ^{15}N/^{13}C frequency ratios (*29*) and the chemical shift of TMS relative to DSS [+1.7 ppm (*30*)]. All shifts have an uncertainty of 0.4 ppm.

The REDOR (*31*) pulse sequence employed to recouple heteronuclear dipolar interactions is shown in Figure 3. The initial S-spin magnetization was created via ramped cross-polarization (*32*) from ^{1}H. The S-spin was observed as a spin−echo, where the echo intensity was modulated due to I−S dipolar interactions reintroduced under MAS by the rotor-synchronized π pulses applied to the I spins. To account for relaxation effects, reference spin−echo spectra were acquired in the absence of I-spin pulses. The I and S radio frequency fields during REDOR were ~40 kHz, and the pulses on the I channel were phased according to the xy-8 scheme (*33*) to compensate for pulse imperfections. CW ^{1}H decoupling (~100 kHz) was applied during the REDOR period, and TPPM decoupling (*34*) (~95 kHz) was used during the acquisition of the free induction decay. For each bR photocycle intermediate studied, REDOR experiments were performed for three mixing times (9.6, 12.8, and 16.0 ms). The data were acquired in blocks of 320 scans, and approximately 14 000 transients were accumulated for each time point. The recycle delay was 2 s.

Internuclear Distances. Experimental ^{13}C REDOR data were analyzed by calculating dephasing ratios for each mixing time, using difference spectroscopy to eliminate the natural-abundance ^{13}C signals from each spectrum. S and S_0 intensities were obtained from the difference spectra by least-squares fits of the retinal 20-^{13}C peak to Gaussian line shapes. The variation of the experimental $(S_0 - S)/S_0 = \Delta S/S_0$ with mixing time was fit to the analytical expression describing the evolution of the observable S spin magnetization (^{13}C in this case) under the REDOR pulse sequence (*31*):

$$\Delta S/S_0(\tau) = \lambda\{1 - \langle\cos(\omega_{IS}\tau)\rangle\} \quad (1)$$

where $\langle\cdots\rangle$ represents averaging over all possible orientations of the I−S dipole vector in the powder sample. The scaling factor λ accounts for the contribution to the S_0 curve from ^{13}C nuclei not dephased by ^{15}N (^{15}N labeling of Trp residues in the sample used for the REDOR experiments was 63%, i.e., $\lambda = 0.63$). ω_{IS} is the orientation-dependent dipolar coupling, which is a function of the dipolar coupling constant, b_{IS} (*35*):

$$b_{IS} = -\left(\frac{\mu_0}{4\pi}\right)\frac{\gamma_I\gamma_S\hbar}{r_{IS}^3} \quad (2)$$

Here, r_{IS} is the I−S internuclear distance and γ_I and γ_S are the gyromagnetic ratios characteristic of the I and S spins, respectively.

RESULTS

^{15}N Chemical Shifts of Trp Model Compounds. To help interpret the ^{15}N spectra of tryptophan residues in bR, we have measured the indole ^{15}N chemical shifts in five natural-abundance tryptophan-containing crystals. The crystallographic studies indicate that the indole nitrogen ($N_{\epsilon 1}$) is hydrogen bonded to an oxygen in Trp-Gly-Gly·2H_2O (*20*), Ac-Trp-OMe (*21*), and L-tryptophan picrate (*22*), and is not hydrogen bonded in *N*-methyl-L-tryptophan (*23*) and Trp·HBr (*24*). We find a ^{15}N chemical shift range of 133.5−125.6 ppm for the H-bonded $N_{\epsilon 1}$, and 127.5−122.3 ppm for the non-H-bonded $N_{\epsilon 1}$. The relatively deshielded nitrogen (127.5 ppm) in Trp·HBr could perhaps be due to very short contacts (3.42−3.80 Å) between $N_{\epsilon 1}$ and four carbons of adjacent indole rings. Figure 4 shows the correlation between the $N_{\epsilon 1}\cdots O$ distance for the H-bonded indoles and the measured $^{15}N_{\epsilon 1}$ chemical shift. We have tentatively assigned the two points for Trp picrate to conform with the overall trend. Consistent with Shoji et al. (*36*), we find that stronger H-bonding correlates with a less shielded ^{15}N nucleus. This correlation suggests the possibility of interpreting tryptophan $^{15}N_{\epsilon 1}$ chemical shifts in terms of H-bond strengths. A linear regression analysis of the data gives the relationship:

$$r_{NO} = -0.0424\ (\text{Å/ppm})\cdot\sigma_N + 8.46\ (\text{Å}) \quad (3)$$

shown by the dashed line in Figure 4.

^{15}N CPMAS Spectra of the Trp Side Chains in bR Photocycle Intermediates. We proceed by considering the ^{15}N indole resonances of the eight tryptophan residues in bR. The ^{15}N CPMAS spectra of [ϵ_1-^{15}N]Trp-bR for the LA,

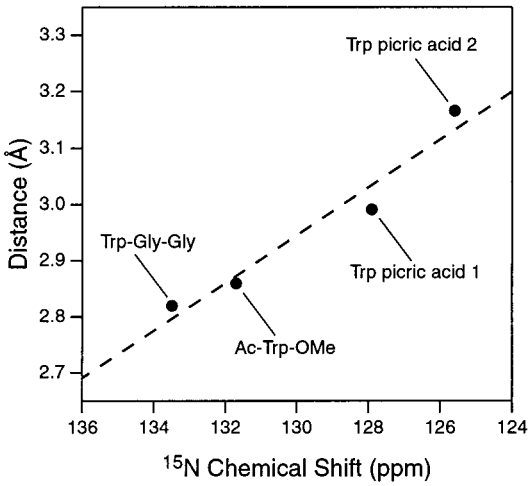

FIGURE 4: N···O hydrogen bond distance vs indole-^{15}N chemical shift in tryptophan-containing crystals with hydrogen-bonded indole nitrogens. The assignment of the two Trp picrate points is tentative since we cannot distinguish between the two sites based on our data.

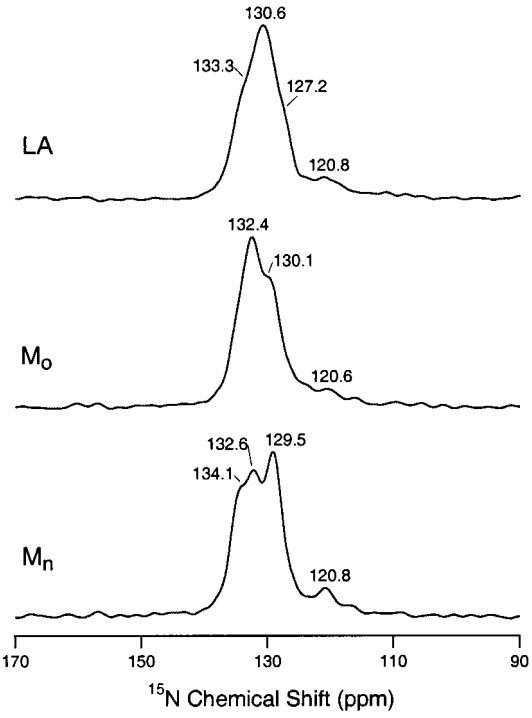

FIGURE 5: ^{15}N CPMAS spectra of [*indole*-^{15}N]Trp-bR intermediates in 0.3 M Gdn-HCl at pH 10.

M_o, and M_n states are shown in Figure 5. In the LA state (Figure 5, top), we observe an unresolved broad envelope of ^{15}N signals ranging from 117 to 137 ppm. The larger peak centered at 130.6 ppm, with a downfield shoulder at 133.3 ppm and an upfield shoulder at 127.2 ppm, corresponds to the ^{15}N signals of the eight labeled indole rings. The low intensity peak centered at 120.8 ppm represents the amide backbone signals due to the ^{15}N natural abundance (and perhaps some scrambling of the original label). Changes in the indoles are apparent in the M_o state (Figure 5, middle), where the maximum intensity is shifted from 130.6 to 132.4 ppm, and a pronounced upfield shoulder is observed at 130.1 ppm. Yet a different ^{15}N profile is acquired for the M_n state (Figure 5, bottom). We identify the most intense peak at

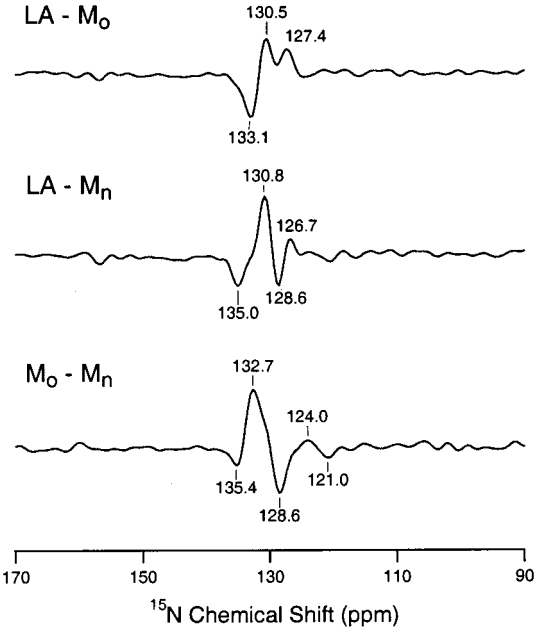

FIGURE 6: Difference ^{15}N CPMAS spectra of [*indole*-^{15}N]Trp-bR intermediates.

129.5 ppm, another peak at 132.6 ppm, and a shoulder on the downfield side at 134.1 ppm.

Since fitting the signals of the eight tryptophans is a nontrivial task, we try to identify the changes between the photocycle intermediates from the CP difference spectra (Figure 6). A careful examination of these spectra suggests that at least three residues are involved in the chemical shift changes between the states. The LA minus M_o spectrum (Figure 6, top) shows positive peaks at 130.5 and 127.4 ppm (LA), and a doubly intense negative peak at 133.1 ppm (M_o). Thus, at least two resonances shift downfield (suggesting stronger H-bonding) in the LA→M_o transition. The LA minus M_n spectrum (Figure 6, middle) shows a doubly intense positive peak at 130.8 ppm (LA) and negative peaks both upfield and downfield at 135.0 and 128.6 ppm (M_n).

^{15}N Chemical Shifts of the Trp182 Side Chain in bR Photocycle Intermediates. One might expect that the perturbations that we see in the ^{15}N CP difference spectra (Figure 6) are most likely to be due to the tryptophans closest to the retinal, i.e., Trp86, Trp138, Trp182, and Trp189. In particular, Trp182 can be considered a likely candidate, since it has been suggested to interact with the C_9 and C_{13} methyl groups of the retinal, and affect different steps of the photocycle (*17*−*19*, *37*). Therefore, we direct our interest to Trp182, and will select the indole nitrogen signal of Trp182 (among the eight indole nitrogens) via its dipolar interaction with the ^{13}C in the C_{13} methyl group, i.e., the C_{20} of the retinal. Since Trp182 is the only tryptophan residue near the C_{13} and C_9 methyl groups of the chromophore, we expect only the ϵ_1-^{15}N of Trp182 and the 20-^{13}C of retinal to be recoupled by REDOR in our sample. As a result, the ^{15}N resonance of the Trp182 indole nitrogen should be isolated by subtracting the ^{15}N REDOR signals from the ^{15}N echo signals of [20-^{13}C]ret,[ϵ_1-^{15}N]Trp-bR (Figure 7). As expected, a single resonance is detected in each photocycle intermediate. The Trp182 $N_{\epsilon 1}$ signal appears at 130.4 ppm in the LA state (Figure 7, top), and shifts to 131.7 ppm in M_o (Figure 7, middle) and to 131.2 ppm in M_n (Figure 7, bottom). As these

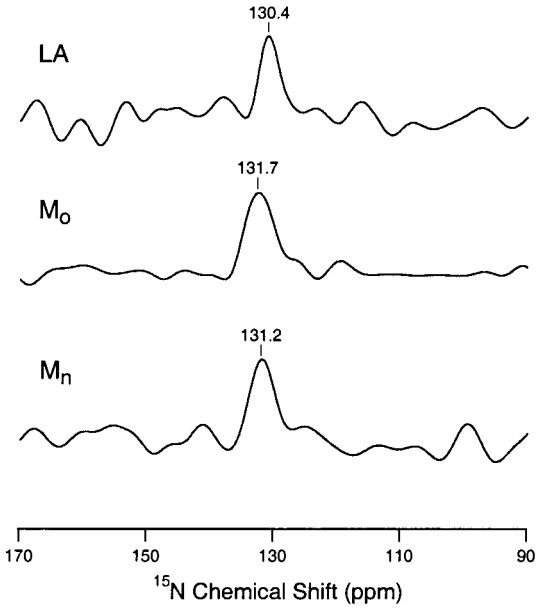

FIGURE 7: ^{15}N REDOR-difference ($S_0 - S$) spectra of [20-^{13}C]-retinal,[*indole*-^{15}N]Trp-bR isolate the ^{15}N signal of the indole nitrogen of Trp182 at 130.4 ppm in LA (top), 131.7 ppm in M_o (middle), and 131.2 ppm in M_n (bottom). The mixing time was 16.0 ms.

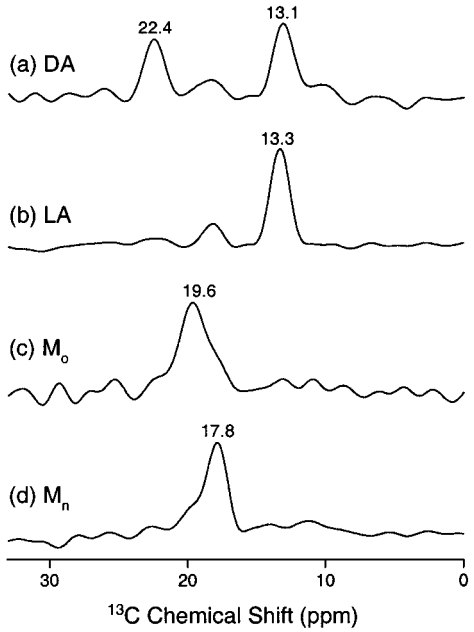

FIGURE 8: ^{13}C resonances of C_{20} of the retinal obtained by subtracting the ^{13}C spectrum of a natural-abundance sample from the spectrum of [20-^{13}C]ret,[ϵ_1-^{15}N]Trp-bR for each intermediate.

results show, the $N_{\epsilon 1}$ chemical shift of Trp182 in M_o and M_n is shifted slightly downfield compared to the LA state. Reference to Figure 4 suggests that in all three states, the indole of Trp182 is moderately strongly hydrogen bonded, perhaps a bit more so in M_o and M_n than in LA. However, it appears that Trp182 is not responsible for the peaks observed in the ^{15}N CP difference spectra (Figure 6).

^{13}C Chemical Shift of the Retinal C_{20} in bR Photocycle Intermediates. Since the retinal isomerization during the LA to M_o and M_n transition does not influence the $N_{\epsilon 1}$ chemical shift of Trp182 substantially, and because the efficiency of the ^{13}C channel of our NMR probe is much higher than the ^{15}N channel, we look for a better marker of the bR state in the C_{20} resonance of the retinal. Figure 8 shows the retinal 20-^{13}C signals obtained for each photocycle intermediate when the ^{13}C spectrum of natural-abundance bR is subtracted from the ^{13}C spectrum of [20-^{13}C]ret,[ϵ_1-^{15}N]Trp-bR. As expected two C_{20} signals are present in the dark-adapted state of bR (Figure 8a) and only one in the light-adapted state (Figure 8b). Signals at ~13.1 ppm for the all-*trans*,15-*anti*-retinal of bR_{568} and at 22.4 ppm for the 13-*cis*,15-*syn*-retinal of bR_{555} are in agreement with the results obtained by Smith et al. (*38*). The upfield shift in bR_{568} relative to bR_{555} is attributed to the steric interaction between the protons of C_{20} and the proton of C_{15} in the all-trans species that is absent in the 13-cis species. The C_{20} signal shifts to 19.6 ppm in M_o (Figure 8c) and to 17.8 ppm in M_n (Figure 8d). Thus, the shift of the C_{20} signal is a convenient marker of bR states. The similarity of the shifts in the two M species suggests that steric interactions of the C_{20} group are not much affected by the relaxation from M_o to M_n, although the interactions seem to be somewhat stronger than in the 13-*cis*-bR_{555}.

Internuclear Distances in bR Photocycle Intermediates. We have employed the REDOR experiment to determine the C_{20}-retinal to $N_{\epsilon 1}$-Trp182 distances for the LA and early M (M_o) photocycle intermediates. Figure 9 shows the ^{13}C spin−echo reference (S_0) (Figure 9a), REDOR dipolar

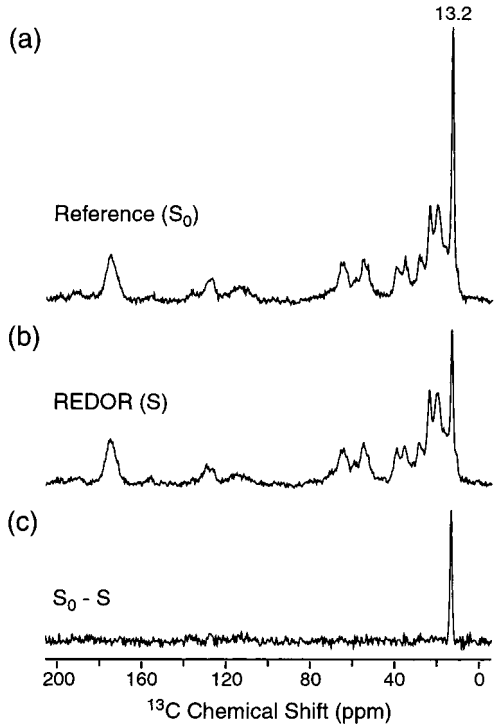

FIGURE 9: REDOR spectra of the light-adapted state of [20-^{13}C]-ret,[ϵ_1-^{15}N]Trp-bR for the mixing time $\tau = 12.8$ ms: (a) ^{13}C spin−echo reference (S_0), (b) REDOR dipolar dephasing (S), and (c) difference ($S_0 - S$).

dephasing (S) (Figure 9b), and difference ($S_0 - S$) (Figure 9c) spectra of [20-^{13}C]retinal,[ϵ_1-^{15}N]Trp-bR in the LA state for the mixing time of 12.8 ms. The 13.2 ppm resonance which corresponds to the retinal C_{20} is prominent in the reference spectrum (Figure 9a), and its intensity is substantially reduced in the REDOR spectrum (Figure 9b), due to dipolar dephasing by the $^{15}N_{\epsilon 1}$ of Trp182.

Similar spectra (not shown) have been obtained for various mixing times for both the LA and M_o states. The resulting

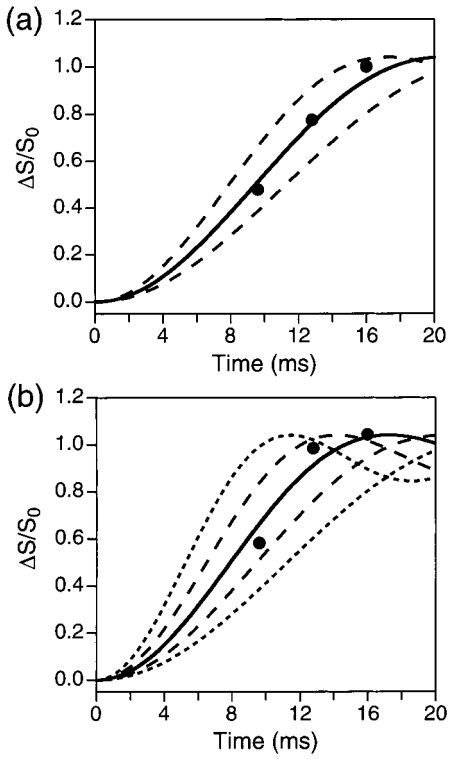

FIGURE 10: $\Delta S/S_0$ REDOR curves for the LA (a) and M_o (b) states of [20-^{13}C]ret,[ϵ_1-^{15}N]Trp-bR. For each state, the experimental points (filled circles) and best-fit simulated $\Delta S/S_0$ curves (solid lines) are shown. The best-fit for the $^{13}C-^{15}N$ distance is 3.36 Å for LA and 3.16 Å for M_o. Also shown are simulations corresponding to the best-fit distance ±0.2 Å (dashed lines) and ±0.4 Å (dotted lines). At the 95% confidence level, the uncertainty in the internuclear distance is ±0.2 Å for LA and ±0.4 Å for M_o.

dephasing ratios are shown in Figure 10. The data suggest faster dephasing in the M_o state than in the LA state, corresponding to a shorter internuclear distance in M_o than in LA. A quantitative estimate of the [20-^{13}C]ret−[ϵ_1-^{15}N]-Trp distance was extracted for each photocycle intermediate by a least-squares fit of the dipolar coupling constant, b_{IS}, to the dephasing data. The resulting distances are 3.36 ± 0.2 Å for LA and 3.16 ± 0.4 Å for M_o, where the uncertainties are given at the 95% confidence level.

DISCUSSION

One of the interesting and critical features of the protonmotive photocycle of bR is that the SB remains connected to the extracellular transport channel after the initial isomerization of the retinal chromophore. This connection appears to be maintained at the cost of distortion of the chromophore. SSNMR (*39*), FTIR (*40*−*43*), and resonance Raman (*44*) spectroscopy find distortion of the chromophore in the L intermediate which is gone in the N intermediate, where the SB connectivity has changed to the intracellular transport channel. The connection of the SB to the extracellular transport channel is not only maintained in L; it is strengthened. The ^{15}N chemical shift of the SB indicates that its interaction with its counterion is considerably stronger in the L state than in the LA state (*39*). (By comparison, the counterion interaction in the N state is weaker than in the L state but stronger than in the LA state.) The electrostatic interaction with the counterion disappears when the SB deprotonates, and release of this constraint may allow the chromophore to relax and the SB to be reoriented toward the intracellular transport channel. This timing is ideal for a protonation switch, the spring-loaded chromophore unwinding immediately after deprotonation, so that reprotonation must occur from a different direction.

The unwinding of the deprotonated chromophore is not entirely unimpeded, however. Two different M states are found when bR is illuminated and relaxed at different temperatures, indicating a significant kinetic barrier from one to the other (*11*, *45*−*47*). In this step, from early M to late M, the distortions in the chromophore relax (*12*), and the SB nitrogen becomes more shielded, indicating greater readiness to reprotonate (*11*). In addition, some perturbations in the peptide backbone of the protein relax, while new perturbations appear elsewhere (*11*). Such adjustments may be responsible for the substantial kinetic barrier of the transition.

In the present work, we have found a similar pattern for the tryptophan residues. Again, perturbations are found in the early M (M_o) state, some of which relax in the transition to late M (M_n) while new perturbations arise. As seen in Figure 6, the activity seems to involve two or three indoles that have moderate hydrogen bonding strengths (ϵ_1-^{15}N resonances at 130.5−130.8 ppm, close to the most common value of 130.6 ppm) in the LA state and one indole that is relatively weakly hydrogen bonded (ϵ_1-^{15}N resonance at 127.4 ppm) in the LA state. The indole that is relatively weakly hydrogen bonded in LA (ϵ_1-^{15}N resonance at 127.4 ppm) is quite tightly hydrogen bonded in M_o (ϵ_1-^{15}N resonance at 133.1 ppm), but no longer perturbed in M_n. On the other hand, whereas only one of the indoles that is moderately hydrogen bonded in LA (ϵ_1-^{15}N resonances at 130.5−130.8 ppm) is perturbed in M_o (ϵ_1-^{15}N resonance at 133.1 ppm), two such indoles are perturbed in M_n (ϵ_1-^{15}N resonances at 135.0 and 128.6 ppm). In M_o, both of the perturbed indoles have become more strongly hydrogen bonded. In M_n, one indole hydrogen bond becomes stronger (in fact exceptionally so), and one becomes weaker.

With its proximity to the C_{13} methyl group of the retinal, Trp182 seemed likely to be perturbed by the bending of the chromophore when it isomerizes around the C_{13}═C_{14} bond. However, by ^{15}N REDOR difference spectroscopy (Figure 7), we have shown that the indole nitrogen of Trp182 is moderately hydrogen bonded in the LA state (ϵ_1-^{15}N resonance at 130.4 ppm), and remains so in the M_o state (ϵ_1-^{15}N resonance at 131.7 ppm) and the M_n state (ϵ_1-^{15}N resonance at 131.2 ppm). Thus, if the hydrogen bonding of Trp182 is perturbed by bending of the chromophore, this perturbation has largely dissipated by the early M state, and the transition from the early M state to the late M state occurs with essentially no effect on the hydrogen bonding of Trp182. These results are consistent with FTIR, UV, and visible Resonance Raman studies (*17*, *19*) which show moderately strong H-bonding between $N_{\epsilon 1}$ of Trp182 and a water molecule in the LA state which is absent in the L state and recovered in the M state. In any case, none of the large perturbations identified by ^{15}N NMR difference spectroscopy (Figure 6) are due to Trp182.

Using the linear regression obtained from the model compound data (Figure 4), hydrogen bond lengths for the indole nitrogens can be estimated from their ^{15}N chemical shifts and compared with the hydrogen bond lengths found

Table 1: Hydrogen Bond Lengths (in Å) for Indole Nitrogens in bR

Trp	nearest oxygen	1C3W	1QHJ
10	CO of Thr5 (1C3W) or Arg7 (1QHJ)	3.52	4.25
12	γ CO of Asn202	3.49	3.40
80	CO of Tyr64	3.45	3.54
86	water	3.41	3.37
137	water	2.78	2.75
138	CO of Pro186	2.94	2.97
182	water	2.81	3.00
189	OH of Tyr83	2.86	2.83

by diffraction (listed in Table 1 for two relatively high-resolution structures). For Trp182, at 130.4 ± 0.4 ppm in the LA state (top panel of Figure 7), we estimate a hydrogen bond length of 2.928 ± 0.04 Å. This compares well with 2.81 Å in the 1C3W diffraction structure and 3.00 Å in the 1QHJ diffraction structure for the distance between the Trp182 indole nitrogen and the oxygen of the hydrogen bonded water. For the downfield shoulder at 133.3 ± 0.4 ppm in the ^{15}N spectrum of the LA state (Figure 5), we estimate a minimum hydrogen bond distance of 2.805 ± 0.04 Å. This also compares well with the shortest indole hydrogen bond distance found in recent diffraction structures—that of Trp137 with water at 2.78 Å in the 1C3W structure and 2.75 Å in the 1QHJ structure. These congruences are encouraging considering the limited resolution of the diffraction and the approximate nature of the interpretation of the ^{15}N chemical shifts. However, divergence occurs for the other end of the spectrum. For the upfield shoulder at 127.2 ± 0.4 ppm, we estimate a maximum hydrogen bond distance of 3.064 ± 0.04 Å. In contrast, in both the 1C3W and the 1QHJ structures, half of the indole nitrogens are more than 3.350 Å from the nearest identifiable hydrogen bond acceptor (see Table 1). For these residues to have nitrogen chemical shifts >127 ppm requires that either they are more tightly hydrogen bonded than the diffraction structures indicate or they experience a special deshielding influence such as we infer for Trp·HBr.

Assuming that, in any case, half of the indole hydrogen bonds are relatively loose, then the other half of the indoles must be presumed responsible for the changes that we see in the LA→M_n transition (middle panel of Figure 6). Of these, Trp138, Trp182, and Trp189 are part of the retinal binding pocket, and Trp137 is not. However, we have already determined that Trp182 is hardly perturbed in M_n (Figure 7). Therefore, we tentatively consider that, of the remaining three tryptophan residues, Trp137, Trp138, and Trp189, the most tightly hydrogen bonded one corresponds to the downfield shoulder in the spectrum and is not perturbed in either M_o or M_n, while the other two correspond to the two moderately hydrogen bonded indoles that are perturbed in M_n, of which one must also be perturbed in M_o. It is tempting to try to assign these residues further with Trp137 at 133.3 ppm based on an r_{NO} of 2.78 Å in 1C3W, with Trp138 at 130.5 ppm based on an r_{NO} of 2.94 Å in 1C3W, and with Trp189 at 131.1 ppm based on an r_{NO} of 2.86 Å in 1C3W. In this scheme, the hydrogen bond between Trp137 and water is unperturbed in M_o and M_n, the hydrogen bond between Trp138 and the C═O of Pro186 becomes tighter in M_o and is altered again in the M_o→M_n transition, and the hydrogen bond betweenTrp189 and the OH of Tyr83 is unperturbed in M_o but is perturbed in the M_o→M_n transition. This is satisfying in that the active residues are the ones that are part of the retinal binding pocket. Unfortunately, however, although the chemical shift variation for these three indoles (133.3−130.5 ppm) is outside the error bars of the NMR experiment, the variation in the hydrogen bond lengths (2.75−2.97 Å) is probably within the error bars of the diffraction experiments and therefore not suitable for making convincing distinctions and assignments.

Table 2: Distance from [20-^{13}C]Retinal to [*indole*-^{15}N]W182 in bR

	resolution (Å)	distance in LA (Å)	distance in photocycle intermediates (Å)
NMR, WT[a]		3.36 ± 0.2	3.16 ± 0.4 (M_o)
simulations, WT[b]			
Scharnagl et al.		4.02	3.57 (L)→3.42 →3.43→3.42 →3.48→3.18 (N)
Schulten et al.		3.66	3.73 or 3.47 (L)
diffraction, WT[c]			
2BRD (*14*)	3.5	3.66	
1BM1 (*50*)	3.5	3.47	
1FBB (*51*)	3.2	3.78	
2AT9 (*52*)	3.0	3.57	
1BRR (*53*)	2.9	3.75, 3.45, 3.58	
1QM8[e]	2.5	3.41	
1DZE[f]	2.5		3.00 (M)
1BRX (*54*)	2.3	3.84	
1CWQ[d]	2.25	3.47	3.41 (M)
1QKP (*55*)	2.1	3.36	
1QKO (*55*)	2.1		2.79 (K)
1EOP (*56*)	2.1	3.27	3.25 (L)
1QHJ (*57*)	1.9	3.27	
1C3W (*58*)	1.55	3.35	
diffraction, D96G/F171C/F219L[c]			
1FBK (*51*)	3.2	3.61	
diffraction, E204Q[c]			
1F5O (*59*)	1.7	3.31	
1F4Z (*59*)	1.8		3.08 (M)
diffraction, D96N[c]			
1C8R (*60*)	1.8	3.17	
1C8S (*60*)	2.0		3.55 (M)

[a] Derived from the present REDOR recoupling experiments. [b] Coordinates kindly supplied by the principal investigators. [c] Structures are from the Protein Data Bank. [d] Sass et al., to be published. [e] Takeda et al., to be published. [f] Takeda et al., to be published.

More exact distances can be obtained from measurements of the dipolar interactions between magnetic nuclei. By analyzing the REDOR data for [20-^{13}C]retinal,[*indole*-^{15}N]-Trp-bR (Figure 10), we have obtained distances from the C_{20} of retinal to the $N_{\epsilon 1}$ of Trp182 of 3.36 ± 0.2 Å in the LA state and 3.16 ± 0.4 Å in the M_o state. These distances are compared in Table 2 with the results of diffraction and simulation studies. The 3.36 Å distance that we obtain for the LA state is short compared to the distances in the early diffraction structures (and simulations based on those structures), but agrees closely with the distances from more recent studies at improved resolution. Of greater interest is the change in the transition from the LA state to the M_o state. In this transition, isomerization of the retinal from all-trans to 13-cis causes the backbone of the chromophore to become bent. Indeed, an increased tilt (~11°) of the C_5 to C_{13} part of the polyene chain out of the plane of the membrane has been detected in the M state by linear dichroism and neutron-diffraction (*48*, *49*). The result could be to push the C_{20} of retinal toward Trp182. In fact, the one diffraction structure

of the K intermediate suggests that such compression does occur, with a [20-^{13}C]retinal−[*indole*-^{15}N]Trp182 distance of just 2.79 Å. However, other diffraction structures suggest less compression in subsequent intermediates. In the present NMR study, the REDOR results suggest that slight compression remains in the M_o state. Although our 95% confidence limits for the M_o state cover the entire range of the diffraction results for photocycle intermediates as well as the range for our LA distance, direct comparison of the most critical data points (see Figure 10) indicates that it is likely that the [20-^{13}C]retinal−[*indole*-^{15}N]Trp182 distance is a bit shorter in the M_o state than in the LA state. Still, the difference is small.

CONCLUSIONS

Using solid-state ^{15}N NMR, we have studied the interactions of the side chains of the eight tryptophan residues in bR and have observed changes in these interactions in the LA→M_o and M_o→M_n transitions of the proton-motive photocycle.

The chemical shifts of the indole nitrogens indicate that they are probably all hydrogen bonded. The indole nitrogen that resonates furthest downfield (and therefore is probably the most strongly hydrogen bonded) in the LA state is unperturbed in the M_o and M_n states. The indole nitrogen that resonates the furthest upfield (and therefore is probably the least strongly hydrogen bonded) in the LA state moves far downfield in the M_o state (and therefore has probably become tightly hydrogen bonded), but relaxes completely in the M_o→M_n transition. At least two other residues are perturbed in the M_n state, one of which is unperturbed in the M_o state and the other of which is differently perturbed in the M_o state. None of these perturbations in indole hydrogen bonding are attributable to Trp182. But other residues in the retinal binding pocket appear to be involved.

We have also measured the internuclear distance between C_{20} of the retinal and $N_{\epsilon 1}$ of Trp182 in the LA and M_o states. The results suggest a slight compression, but the change in distance, from 3.36 ± 0.2 to 3.16 ± 0.4 Å, is too small to be reliably distinguished. From the M_o state to the M_n state, the 1.8 ppm upfield shift in the [20-^{13}C]retinal resonance suggests a slight increase in compression, but again it is very small.

ACKNOWLEDGMENT

We thank Prof. C. Scharnagl and Prof. K. Schulten for sharing the coordinates of simulated photocycle intermediates. Thanks are also accorded to David Ruben and Chad Rienstra for technical assistance and advice, and to Brett Tounge and Jon Lansing for stimulating discussions.

REFERENCES

1. Lanyi, J. K. (1993) *Biochim. Biophys. Acta 1183*, 241−261.
2. Maeda, A. (1995) *Isr. J. Chem. 35*, 387−400.
3. Haupts, U., Tittor, J., and Oesterhelt, D. (1999) *Annu. Rev. Biophys. Biomol. Struct. 28*, 367−399.
4. Scharnagl, C., Hettenkofer, J., and Fischer, S. F. (1995) *J. Phys. Chem. 99*, 7787−7800.
5. Zhou, F., Windemuth, A., and Schulten, K. (1993) *Biochemistry 32*, 2291−2306.
6. Xu, D., Sheves, M., and Schulten, K. (1995) *Biophys. J. 69*, 2745−2760.
7. Varo, G., and Lanyi, J. K. (1991) *Biochemistry 30*, 5008−5015.
8. Varo, G., and Lanyi, J. K. (1991) *Biophys. J. 59*, 313−322.
9. Radionov, A. N., Klyachko, V. A., and Kaulen, A. D. (1999) *Biochemistry (Moscow) 64*, 1210−1214.
10. Hessling, B., Herbst, J., Rammelsberg, R., and Gerwert, K. (1997) *Biophys. J. 73*, 2071−2080.
11. Hu, J. G., Sun, B. Q., Bizounok, M., Hatcher, M. E., Lansing, J. C., Raap, J., Verdegem, P. J. E., Lugtenburg, J., Griffin, R. G., and Herzfeld, J. (1998) *Biochemistry 37*, 8088−8096.
12. Hatcher, M. E., Hu, J. G., Belenky, M., Verdegem, P., Lugtenburg, J., Griffin, R. G., and Herzfeld, J. (2002) *Biophys. J.* (in press).
13. Henderson, R., Baldwin, J. M., Ceska, T. A., Zemlin, F., Beckmann, E., and Downing, K. H. (1990) *J. Mol. Biol. 213*, 899−929.
14. Grigorieff, N., Ceska, T. A., Downing, K. H., Baldwin, J. M., and Henderson, R. (1996) *J. Mol. Biol. 259*, 393−421.
15. Hatanaka, M., Kashima, R., Kandori, H., Friedman, N., Sheves, M., Needleman, R., Lanyi, J. K., and Maeda, A. (1997) *Biochemistry 36*, 5493−5498.
16. Tajkhorshid, E., Baudry, J., Schulten, K., and Suhai, S. (2000) *Biophys. J. 78*, 683−693.
17. Yamazaki, Y., Sasaki, J., Hatanaka, M., Kandori, J., Maeda, A., Needleman, R., Shinada, T., Yoshihara, K., Brown, L. S., and Lanyi, J. K. (1995) *Biochemistry 34*, 577−582.
18. Weidlich, O., Schalt, B., Friedman, N., Sheves, M., Lanyi, J. K., Brown, L. S., and Siebert, F. (1996) *Biochemistry 35*, 10807−10814.
19. Hashimoto, S., Obata, K., Takeuchi, H., Needleman, R., and Lanyi, J. K. (1997) *Biochemistry 36*, 11583−11590.
20. Subramanian, E., and Sahayamary, J. J. (1989) *Int. J. Pept. Protein Res. 34*, 134−138.
21. Cotrait, P. M., and Barrans, Y. (1974) *Acta Crystallogr. B30*, 510−513.
22. Ishida, T., Nagata, H., In, Y., Doi, M., Inoue, M., Extine, M. W., and Wakahara, A. (1993) *Chem. Pharm. Bull. 41*, 433−438.
23. Seetharaman, J., Rajan, S. S., and Srinivasan, R. (1993) *J. Crystallogr. Spectrosc. Res. 23*, 167−170.
24. Takigawa, T., Ashida, T., Sasada, Y., and Kakudo, M. (1966) *Bull. Chem. Soc. Jpn. 39*, 2369−2378.
25. Pardoen, J. A., Neijenesch, H. N., Mulder, P. P. J., and Lugtenburg, J. (1983) *Recl. Trav. Chim. Pays-Bas 102*, 341−347.
26. Gochnauer, M. B., and Kushner, D. J. (1969) *Can. J. Microbiol. 15*, 1157−1165.
27. Oesterhelt, D., and Stoeckenius, W. (1974) *Methods Enzymol. 31*, 667−678.
28. Earl, W. L., and VanderHart, D. L. (1982) *J. Magn. Reson. 48*, 35−54.
29. Markley, J. L., Bax, A., Arata, Y., Hilbers, C. W., Kaptein, R., Sykes, B. D., Wright, P. E., and Wüthrich, K. (1998) *Pure Appl. Chem. 70*, 117−142.
30. Wishart, D. S., Bigam, C. G., Yao, J., Abildgaard, F., Dyson, H. J., Oldfield, E., Markley, J. L., and Sykes, B. D. (1995) *J. Biomol. NMR 6*, 135−140.
31. Gullion, T., and Schaefer, J. (1989) *J. Magn. Reson. 81*, 196−200.
32. Metz, G., Wu, X., and Smith, S. O. (1994) *J. Magn. Reson., Ser. A 110*, 219−227.
33. Gullion, T., Baker, D. B., and Conradi, M. S. (1990) *J. Magn. Reson. 89*, 479−484.
34. Bennett, A. E., Rienstra, C. M., Auger, M., Lakshmi, K. V., and Griffin, R. G. (1995) *J. Chem. Phys. 103*, 6951−6957.
35. Mehring, M. (1983) *Principles of High-Resolution NMR in Solids*, Springer-Verlag, Berlin.
36. Shoji, A., Ando, S., Kuroki, S., Ando, I., and Webb, G. A. (1993) in *Annual Reports on NMR Spectroscopy*, pp 55−98, Academic Press, London.
37. Gärtner, W., Towner, P., Hopf, H., and Oesterhelt, D. (1983) *Biochemistry 22*, 2637−2644.

38. Smith, S. O., de Groot, H. J. M., Gebhard, R., Courtin, J. M. L., Lugtenburg, J., Herzfeld, J., and Griffin, R. G. (1989) *Biochemistry 28*, 8897−8904.
39. Hu, J. G., Sun, B. Q., Petkova, A. T., Griffin, R. G., and Herzfeld, J. (1997) *Biochemistry 36*, 9316−9322.
40. Fahmy, K., Siebert, F., Grossjean, M. F., and Tavan, P. (1989) *J. Mol. Struct. 214*, 257−288.
41. Maeda, A., Sasaki, J., Pfefferle, J. M., Shichida, Y., and Yoshizawa, T. (1991) *Photochem. Photobiol. 54*, 911−921.
42. Pfefferle, J. M., Maeda, A., Sasaki, J., and Yoshizawa, T. (1991) *Biochemistry 30*, 6548−6556.
43. Weidlich, O., and Siebert, F. (1993) *Appl. Spectrosc. 47*, 1394−1400.
44. Lohrmann, R., and Stockburger, M. (1992) *J. Raman Spectrosc. 23*, 575−583.
45. Vonck, J., Han, B.-G., Burkard, F., Perkins, G. A., and Glaeser, R. M. (1994) *Biophys. J. 67*, 1173−1178.
46. Sass, H. J., Schachowa, I. W., Rapp, G., Koch, M. H. J., Oesterhelt, D., Dencher, N. A., and Büldt, G. (1997) *EMBO J. 16*, 1484−1491.
47. Han, B.-G., Vonck, J., and Glaeser, R. M. (1994) *Biohys. J. 67*, 1179−1186.
48. Heyn, M. P., and Otto, H. (1992) *Photochem. Photobiol. 56*, 1105−1112.
49. Hauss, T., Büldt, G., Heyn, M. P., and Dencher, N. A. (1994) *Proc. Natl. Acad. Sci. U.S.A. 91*, 11854−11858.
50. Sato, H., Takeda, K., Tani, K., Hino, T., Okada, T., Nakasako, M., Kamiya, N., and Kouyama, T. (1999) *Acta Crystallogr., Sect. D 55*, 1251−1256.
51. Subramaniam, S., and Henderson, R. (2000) *Nature 406*, 653−657.
52. Mitsuoka, K., Hirai, T., Murata, K., Miyazawa, A., Kidera, A., Kimura, Y., and Fujiyoshi, Y. (1999) *J. Mol. Biol. 286*, 861−882.
53. Essen, L.-O., Siegert, R., Lehmann, W. D., and Oesterhelt, D. (1998) *Proc. Natl. Acad. Sci. U.S.A. 95*, 11673−11678.
54. Luecke, H., Richter, H.-T., and Lanyi, J. K. (1998) *Science 280*, 1934−1937.
55. Edman, K., Nollert, P., Royant, A., Belrhali, H., Pebay-Peyroula, E., Hajdu, J., Neutze, R., and Landau, E. M. (1999) *Nature 401*, 822−826.
56. Royant, A., Edman, K., Ursby, T., Pebay-Peyroula, E., Landau, E., and Neutze, R. (2000) *Nature 406*, 645−648.
57. Belrhali, H., Nollert, P., Royant, A., Menzel, C., Rosenbusch, J. P., Landau, E. M., and Pebay-Peyroula, E. (1999) *Struct. Fold. Des. 7*, 909−917.
58. Luecke, H., Schobert, B., Richter, H. T., Cartailler, J. P., and Lanyi, J. K. (1999) *J. Mol. Biol. 291*, 899−911.
59. Luecke, H., Schobert, B., Cartailler, J. P., Richter, H. T., Rosengarth, A., Needleman, R., and Lanyi, J. K. (2000) *J. Mol. Biol. 300*, 1237−1255.
60. Luecke, H., Schobert, B., Richter, H.-T., Cartailler, J.-P., and Lanyi, J. K. (1999) *Science 286*, 255−260.

BI012127M